Thin Solid Films 517 (2009) 5130–5133

Contents lists available at ScienceDirect

Thin Solid Films

journal homepage: www.elsevier.com/locate/tsf

Artificial charge modulation in perovskite vanadate superlattices

W.C. Sheets, Ph. Boullay, U. Lüders, B. Mercey, W. Prellier *

Laboratoire CRISMAT, CNRS UMR 6508, ENSICAEN, 6 Blvd Maréchal Juin, F-14050 Caen Cedex, France

ARTICLE INFO

Available online 14 March 2009

Keywords:
Thin films
Oxydes
Superlattices
Metal-insulator transition
Pulsed laser deposition

ABSTRACT

A series of epitaxial $(LaVO_3)_{6m}(SrVO_3)_m$ superlattices having the same nominal composition as $La_{6/7}Sr_{1/7}VO_3$, a Mott–Hubbard insulator, was grown with pulsed-laser deposition on [001]-oriented $SrTiO_3$ substrates, and their superlattice period is varied. When $m=1$, the insulating resistivity of bulk-like $La_{6/7}Sr_{1/7}VO_3$ is obtained; however, an increase in the periodicity ($m\geq 2$) results in metallic samples. Comparison of the superlattice periodicity with the coherence length of charge carriers in perovskite oxide heterostructures is used to understand these observations. A filling-controlled insulator-metal transition is induced by placing a single dopant layer of $SrVO_3$ within $LaVO_3$ layers of varying thickness.

1. Introduction

Thin film methods offer a versatile approach to overcome the natural preference for disorder or low-dimensional ordering in certain materials by controlling the location of cations in tailored oxide multilayers [1]. Fabrication of such heterostructures, composed of different perovskite oxides, has been utilized to explore the change in, for example, the magnetic response, magneto-resistance, and ferroelectric properties [2–4]. Artificial heterostructures have been utilized more recently to probe how interlayer coupling and charge ordering at the interface affect such properties [5–7]. For instance, Ohtomo et al. deposited a single layer of $LaTiO_3$ in a $SrTiO_3$ matrix [8]. This $LaTiO_3/SrTiO_3$ superlattice exhibits metallic conductivity, similar to a bulk solid solution of $La_{1-x}Sr_xTiO_3$, even though the heterostructure is based on two insulators. The spatial distribution of Ti^{3+} across the atomically abrupt $LaTiO_3/SrTiO_3$ interfaces was mapped by electron energy-loss spectroscopy (EELS). Another study on the interface of a $LaVO_3/LaVO_4$ superlattice revealed the presence of a two-dimensional layer of V^{4+} between the two layers, corresponding to a $LaVO_x$ phase with an oxidation state that does not exist in the bulk [9]. It is anticipated, therefore, that an interface between layers of $LaVO_3$ and $SrVO_3$ in a heterostructure will yield a mixed V^{3+} and V^{4+} valence. It is of particular interest to know the length scale of this interaction and its effect on the electrical transport properties of $LaVO_3/SrVO_3$ superlattices, including whether varying the periodicity of such superlattices can induce a filling-controlled transition from a Mott–Hubbard insulating to a metallic state. In this contribution, successful syntheses of varying period superlattices of epitaxial $(LaVO_3)_m(SrVO_3)_n$ thin films, in which the electrical transport properties are affected noticeably by the superlattice period Λ, are presented.

The $(La,Sr)VO_3$ system has been studied extensively owing to its classic filling-controlled insulator-metal transition behaviour [10,11]. The solid solution $La_{1-x}Sr_xVO_3$ exists over the entire composition $(0\leq x\leq 1)$ all the way from $LaVO_3$, a Mott–Hubbard insulator that undergoes an antiferromagnetic (AFM) transition, to $SrVO_3$, a paramagnetic metallic conductor, without disrupting the distorted perovskite structural network. On introducing Sr^{2+} into $LaVO_3$, a mixed V^{3+} and V^{4+} valence occurs, which favors the formation of σ^* and π^* impurity bands whose broadening eventually closes the band gap and results in metallic behaviour [12,13]. The Mott–Hubbard insulating phase disappears at a strontium substitution level of $x>0.2$, and doping with more holes produces a metallic state [11,14–16].

2. Experimental details

The $(LaVO_3)_m(SrVO_3)_n$ superlattice films were deposited on [001]-oriented $SrTiO_3$ using pulsed-laser deposition (PLD) from single phase, ceramic targets of LaVO4 and $Sr_2V_2O_7$. The cubic lattice parameter of the $SrTiO_3$ substrate $a_{STO}=3.905$ Å matches well with the pseudocubic cubic lattice parameter of $LaVO_3$ (LVO), $a_{LVO}=3.92$ Å (Ref. [17]) and cubic lattice parameter of $SrVO_3$ (SVO), $a_{SVO}=3.843$ Å [18]. Superlattices of $(LaVO_3)_m(SrVO_3)$ were grown at a substrate temperature of 700 cC and oxygen pressure of 10–5 Torr, conditions which represented the best compromise for simultaneously stabilizing both SVO and LVO phases in a heterostructure. Several important deposition parameters were KrF excimer laser with $\lambda=248$ nm, pulse rate = 3 Hz, laser power density ≈2 J cm^{-2}, and target to substrate distance = 75 mm. Deposition rates of 0.2 and 0.4 Å/pulse for LVO and SVO, respectively, were calibrated under these conditions. Post-growth the samples were cooled to room temperature under dynamic vacuum (10^{-5} Torr) at a rate of 10 °C min^{-1}. The top layer is always SVO. The crystalline structure of the thin film samples was examined by X-ray diffraction (XRD) using a Seifert 3000P diffractometer (Cu

* Corresponding author.
E-mail address: prellier@ensicaen.fr (W. Prellier).

0040-6090/$ – see front matter © 2009 Elsevier B.V. All rights reserved.
doi:10.1016/j.tsf.2009.03.031

Kα, λ = 1.5406 Å). Transmission electron microscopy (TEM) images were obtained using a JEOL 2010F electron microscope.

3. Results

To probe the length scale of charge screening at the interface between LVO and SVO layers a series of $(LaVO_3)_{6m}(SrVO_3)_m$ thin films samples, where the overall stoichiometry is equal to $La_{0.86}Sr_{0.14}VO_3$, were deposited under identical conditions. Each superlattice consisted of depositing 6*m* integer layers of LVO, followed by *m* integer layers of SVO, repeated in an appropriate sequence, such that the total perovskite unit cells grown is an integer near 350. In addition, a $La_{6/7}Sr_{1/7}VO_3$ sample with a superlattice periodicity $\Lambda < a_p$ (where Λ is the superlattice period and a_p is the perovskite lattice parameter) also was prepared as a reference solid solution sample. Conventional Θ–2Θ scans of the superlattices revealed no extra peaks other than the (00l) Bragg reflections of the substrate, constituent film, and satellites peaks.

The good-quality of the artificially induced cation order is evidenced by the numerous observed satellite peaks (inset Fig. 1) for each sample. The average out-of-plane lattice parameter of the superlattice (a_p) was obtained from the central (001) Bragg peak of the film and the superlattice period (Λ) for each sample was determined from the observed *i*th order peaks about the (001) and (002) film peaks. At low periodicities, the lattice could accommodate the strain, and on increasing the periodicity the strain relaxes and a shift in the average lattice spacing towards that of the $SrTiO_3$ substrate is observed. Fig. 1 illustrates that the measured $(LaVO_3)_{6m}(SrVO_3)_m$ superlattice periods Λ were in good agreement (<3% error) with targeted values. The error in superlattice stacking was quantified by $V = [(\Lambda - (7m \times a_p))/\Lambda] \times 100$. The lattice parameter a_p was consistent for each superlattice of different periodicity, ranging from 3.945 to 3.952 Å; their similarity to each other and that of the solid solution $La_{6/7}Sr_{1/7}VO_3$ argues for constant stoichiometry of the superlattices. At low periodicities, the lattice could accommodate the strain, and on increasing the periodicity the strain relaxes and a shift in the average lattice spacing towards that of the $SrTiO_3$ substrate is observed. A cross-sectional TEM image of a representative $(LVO)_{17}(SVO)_3$ superlattice, viewed along the [001] of $SrTiO_3$ substrate, is shown in Fig. 2. Good interfacial quality and lateral coherency (i.e., no significant discontinuities) of the orthorhombic *Pnma* $LaVO_3$ (darker) and cubic *Pm-3m* $SrVO_3$ (lighter) perovskites are observed. This evidences a highly two-dimensional growth mode,

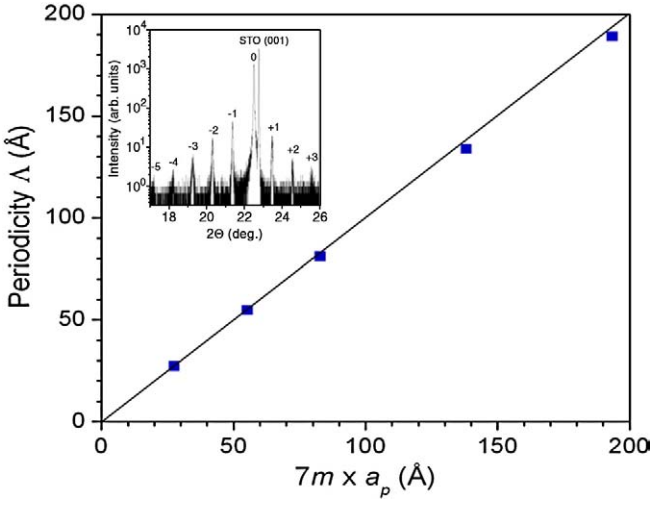

Fig. 1. A plot illustrates the evolution of the calculated periodicity (Λ) as a function of the targeted value ($7m \times a_p$) for several $(LaVO_3)_{6m}(SrVO_3)_m$ superlattices. The line is drawn as a guide to the eye. The inset shows a Θ–2Θ pattern recorded around the (001) reflection of $SrTiO_3$ for a $(LaVO_3)_{18}(SrVO_3)_3$ superlattice with a calculated periodicity of 81.0 Å.

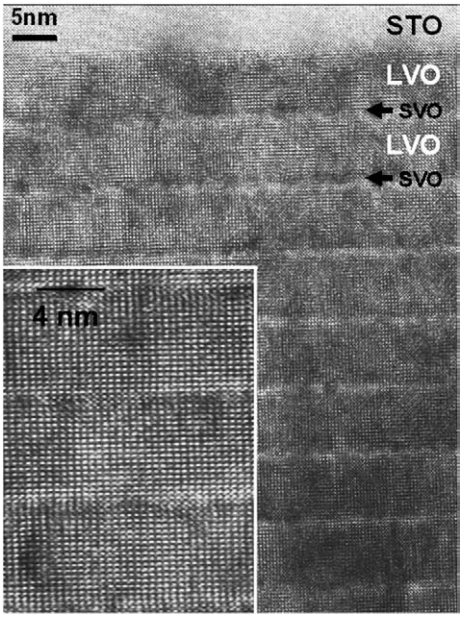

Fig. 2. A cross-section TEM of a $(LaVO_3)_{17}(SrVO_3)_3$ superlattice. The lighter bands are $SrVO_3$ ($3a_p$), the darker bands $LaVO_3$ ($17a_p$). The $SrTiO_3$ substrate is at the top. Inset left is an enlarged image. The scale is indicated.

relatively abrupt interfaces, and artificial cationic order in these superlattices (see inset of Fig. 2). A complete study of the superlattice structural characteristics will be presented elsewhere.

The overall conductivity of the $(LaVO_3)_{6m}(SrVO_3)_m$ multilayers are a function of the spacing between, and thickness of, the dopant $SrVO_3$ layers. The resistivity of these samples transitions systematically from that of a solid solution to bulk-like individual layers with an increase in periodicity. Four-point resistance measurements were measured by a Quantum Design physical property measurement system (PPMS) and the resistivity was calculated from these measurements using the appropriate correction factors for a two-dimensional rectangular sample with finite thickness [19]. Fig. 3(a) shows the temperature-dependent resistivity of the $(LaVO_3)_{6m}(SrVO_3)_m$ superlattices along with thin film samples of LVO, SVO, and solid solution $La_{6/7}Sr_{1/7}VO_3$ ($\Lambda < a_p$) deposited by PLD under the same conditions. No kinks, which signal the occurrence of a first-order structural phase transition from orthorhombic to monoclinic form [16,20], are visible in the resistivity plots of the $(LaVO_3)_{6m}(SrVO_3)_m$ superlattice samples. Suppression of this structural phase transformation for thin film samples of the solid solution $La_{1-x}Sr_xVO_3$ has been reported previously [12]. For $La_{1-x}Sr_xVO_3$ samples where the strontium concentration (x) is equal to 1/7 or 0.14, the expectation from the electronic phase diagram is that these samples should be AFM and Mott–Hubbard insulators at low temperatures [16]. As shown in Fig. 3a, only the $m = 1$ multilayer displays insulating, not metallic, behavior, implying that there is significant interlayer coupling and dispersion of the extra charge carrier within the smallest period heterostructure. Indeed, the magnitude and shape of the resistivity plot for the $m = 1$ superlattice is similar to that measured for the $\Lambda < a_p$ thin film sample, which can be considered to have a statistical distribution of the A-site cations. As mentioned previously, EELS measurements have shown that the charge distribution of an extra charge carrier associated with the single dopant layer naturally spreads beyond the heterostructure interface into the host layers in order to minimize the electronic free energy [8]. At a single $LaTiO_3/SrTiO_3$ interface, the length scale of the charge interaction was measured to be 10 Å for the crossover between valence states, while the total spatial distribution of the dopant charge carriers was ~40 Å. Such distances are consistent with the $m = 1$ multilayer (Λ = 27.2 Å) exhibiting a resistivity similar to that of a solid